# Expression of recombinant human complement C1q allows identification of the C1r/C1s-binding sites

Isabelle Bally[a,b,c], Sarah Ancelet[a,b,c], Christine Moriscot[a,b,c,d], Florence Gonnet[e,f], Alberto Mantovani[g], Régis Daniel[e,f], Guy Schoehn[a,b,c,d], Gérard J. Arlaud[a,b,c], and Nicole M. Thielens[a,b,c,1]

[a]Commissariat à l'Energie Atomique et aux Energies Alternatives, Direction des Sciences du Vivant, Institut de Biologie Structurale, F-38027 Grenoble, France; [b]Centre National de la Recherche Scientifique (CNRS), Unité Mixte de Recherche (UMR) 5075, F-38027 Grenoble, France; [c]Université Grenoble Alpes, F-38000 Grenoble, France; [d]CNRS, Unité Mixte Internationale 3265, Unit for Virus Host Cell Interactions, F-38042-Grenoble, France; [e]CNRS, UMR 8587, Laboratoire Analyse et Modélisation pour la Biologie et l'Environnement, F-91025 Evry, France; [f]Université d'Evry-Val-d'Essonne, Laboratoire Analyse et Modélisation pour la Biologie et l'Environnement, F-91025 Evry, France; and [g]Istituto Clinico Humanitas, Rozzano, 20089 Milan, Italy

Edited* by Douglas T. Fearon, University of Cambridge School of Clinical Medicine, Cambridge, United Kingdom, and approved March 28, 2013 (received for review March 14, 2013)

**Complement C1q is a hexameric molecule assembled from 18 polypeptide chains of three different types encoded by three genes. This versatile recognition protein senses a wide variety of immune and nonimmune ligands, including pathogens and altered self components, and triggers the classical complement pathway through activation of its associated proteases C1r and C1s. We report a method for expression of recombinant full-length human C1q involving stable transfection of HEK 293-F mammalian cells and fusion of an affinity tag to the C-terminal end of the C chain. The resulting recombinant (r) C1q molecule is similar to serum C1q as judged from biochemical and structural analyses and exhibits the characteristic shape of a bunch of flowers. Analysis of its interaction properties by surface plasmon resonance shows that rC1q retains the ability of serum C1q to associate with the C1s-C1r-C1r-C1s tetramer, to recognize physiological C1q ligands such as IgG and pentraxin 3, and to trigger C1r and C1s activation. Functional analysis of rC1q variants carrying mutations of LysA59, LysB61, and/or LysC58, in the collagen-like stems, demonstrates that LysB61 and LysC58 each play a key role in the interaction with C1s-C1r-C1r-C1s, with LysA59 being involved to a lesser degree. We propose that LysB61 and LysC58 both form salt bridges with outer acidic $Ca^{2+}$ ligands of the C1r and C1s CUB (complement C1r/C1s, Uegf, bone morphogenetic protein) domains. The expression method reported here opens the way for deciphering the molecular basis of the unusual binding versatility of C1q by mapping the residues involved in the sensing of its targets and the binding of its receptors.**

C1 complex | innate immunity | protein engineering

C1q is the recognition protein of the classical complement pathway, a major component of the humoral innate immune defense. C1q binds to pathogens either directly or via immune mediators such as antibodies and pentraxins (PTXs), thereby triggering the complement cascade through activation of its associated proteases C1r and C1s (1, 2). Complement activation leads to elimination of the target microorganism through opsonophagocytosis, inflammation, and cytolysis, while instructing an adaptive immune response. Importantly, C1q also detects potentially harmful altered self-components such as apoptotic cells and triggers their safe elimination while stimulating an anti-inflammatory response, thereby contributing to maintenance of host tissue integrity (3, 4). Besides its role in complement activation, C1q is involved in diverse biological functions such as immune cell modulation, blood coagulation, development, reproduction, and in the pathogenesis of numerous diseases, including neurodegenerative disorders and cancer (5, 6). These functions arise from the unusual binding versatility of C1q, which is able to interact with an amazing variety of soluble and cell surface ligands (1).

C1q is a complex molecule assembled from 18 polypeptide chains of three different types (A, B, and C) encoded by three genes (7). Each chain comprises an N-terminal collagen-like sequence and a C-terminal globular gC1q module, with disulfide bonds linking the N-terminal ends of the A and B chains and of two C chains. Each A-B dimer associates noncovalently with a C chain to form a heterotrimeric collagen-like triple helix prolonged by a globular domain (7). The association of six such trimers yields C1q, a 466-kDa protein with the characteristic shape of a bouquet of flowers, comprising six collagen-like triple helices that join together in their N-terminal half to form a "stalk" and then diverge to form individual "stems," each terminating in a C-terminal globular "head."

Whereas the C1q sensing properties are mediated by its globular heads, the collagen-like moiety is responsible for interaction with the $Ca^{2+}$-dependent C1s-C1r-C1r-C1s tetramer, each of these two regions being involved in the binding of C1q to various cell surface receptors (8). The crystal structure of the heterotrimeric C1q head has been solved, providing insights into the versatility of the C1q sensing properties (9). However, precise mapping of the residues involved in target recognition and in the C1s-C1r-C1r-C1s–binding site(s) has been precluded to date because of the fact that, owing to its three-chain structure, C1q could not be produced in a recombinant form. The present study describes production of recombinant full-length human C1q in stably transfected mammalian cells. Its biochemical, physicochemical, and functional analysis shows that it is correctly folded and retains the ability to associate with the C1s-C1r-C1r-C1s tetramer, sense physiological ligands, and trigger activation of C1s-C1r-C1r-C1s. The availability of a method for expressing recombinant C1q opens the way for deciphering the multiple interaction properties of this protein, as illustrated here by the identification by site-directed mutagenesis of the C1s-C1r-C1r-C1s–binding residues in the C1q collagen-like stems.

## Results

**Expression and Purification of WT Recombinant Human C1q.** Different attempts to produce human C1q in a recombinant form were performed initially using transient transfection of CHO cells, but these yielded no evidence for production of recombinant material. HEK 293-F cells were next used as host cells, performing initially transient transfection either by each C1q chain individually or by the three chains simultaneously. In the latter case,

Author contributions: I.B., G.J.A., and N.M.T. designed research; I.B., S.A., C.M., F.G., R.D., G.S., and N.M.T. performed research; A.M. contributed new reagents/analytic tools; I.B., C.M., F.G., R.D., G.S., G.J.A., and N.M.T. analyzed data; and G.J.A. and N.M.T. wrote the paper.

Conflict of interest statement: This work is part of a patent application by I.B. and N.M.T.

*This Direct Submission article had a prearranged editor.

[1]To whom correspondence should be addressed. E-mail: nicole.thielens@ibs.fr.

This article contains supporting information online at www.pnas.org/lookup/suppl/doi:10.1073/pnas.1304894110/-/DCSupplemental.

expression of the three chains could be detected by Western blot analysis, and yet the recombinant material did not bind significantly to IgG–ovalbumin aggregates, providing no evidence for the generation of correctly folded C1q. Several observations suggested that assembly of the C chain was a limiting factor in the assembly of the whole C1q molecule.

Stable HEK 293-F cell lines producing recombinant human C1q were next generated in two steps: (*i*) generation of stable transfectants expressing both the A and B chains; and (*ii*) subsequent transfection of these cells by the C1qC-FLAG DNA construct. The resulting transfectants expressed recombinant (r) C1q molecules, as judged by Western blot analysis, which revealed the presence of characteristic C1q bands in the culture supernatants. To select functional molecules, the recombinant material was initially purified using the affinity of C1q for insoluble IgG–ovalbumin aggregates. This first step led to the recovery of about 50% of the rC1q molecules, suggesting that the remainder, mainly corresponding to high-molecular weight species, was not properly folded. Further purification of rC1q was achieved by chromatography on an anti-FLAG affinity column. Virtually all C1q molecules bound to the column and could be eluted subsequently by the FLAG peptide. This step also allowed us to eliminate contaminating IgG molecules arising from the previous step. The overall procedure allowed routinely production of 0.5–0.8 mg of purified rC1q from 1 L of culture supernatant.

SDS/PAGE analysis of purified rC1q showed a band pattern similar to that of serum-derived C1q with characteristic A-B and C-C dimers under nonreducing conditions (Fig. 1*A*, lanes 1 and 2) and the three A, B, and C chains under reducing conditions (Fig. 1*A*, lanes 3 and 4). Consistent with the addition of the FLAG tag (995 Da), the C-C dimer and the C chain both exhibited significantly higher apparent molecular weights compared with their unmodified counterparts in serum-derived C1q (Fig. 1*A*, lanes 2 and 4).

**Biochemical and Structural Characterization of rC1q.** N-terminal sequence analysis of the three rC1q chains was performed after SDS/PAGE and electrotransfer. The A and C chains each yielded amino acid sequences in agreement with published data (10), namely Glu-Asp-Leu-(Cys)-Arg-Ala-Pro… and Asn-Thr-Gly-(Cys)-Tyr-Gly-Ile-Pro…, respectively. Consistent with the fact that it has a blocked N-terminal amino acid (11), the B chain yielded no detectable sequence.

Mass spectrometric analysis of the reduced rC1q was performed using the MALDI-TOF technique. In keeping with previous analyses (12), serum C1q yielded three well-resolved monocharged peaks corresponding to the individual A, B, and C chains (Fig. 1*B*). In the case of rC1q, in contrast, the mass increment of 995 Da brought about by the FLAG tag caused the C chain to partly overlap with the B chain, resulting in poorly resolved peaks (Fig. 1*C*). Nevertheless, the masses of the B and C chains could be determined from their mono- and doubly-charged ions, yielding values of 25,591 ± 107 and 24,940 ± 109 Da, fully consistent with those of their counterparts in serum C1q (25,589 ± 15 and 24,001 ± 24 Da, respectively), suggesting that both chains had undergone the same posttranslational glycosylations and hydroxylations as occurring in native human C1q. In contrast, the average mass value of the A chain (27,355 ± 58 Da) was consistently found to be lower than that of its counterpart in serum C1q (27,584 ± 40 Da). The difference (229 ± 58 Da) is roughly consistent with the mass of *N*-acetylneuraminic acid (291 Da), suggesting that the N-linked oligosaccharide borne by the A chain was slightly shorter, possibly because of the lack of a terminal sialic acid.

Negative-staining electron microscopy was next used to visualize the rC1q protein using sodium silicotungstate as stain. As illustrated in Fig. 2*A*, well-defined oligomeric molecules were clearly observed. The selected images presented in Fig. 2*B* show both side views and top views of rC1q, in which the six globular

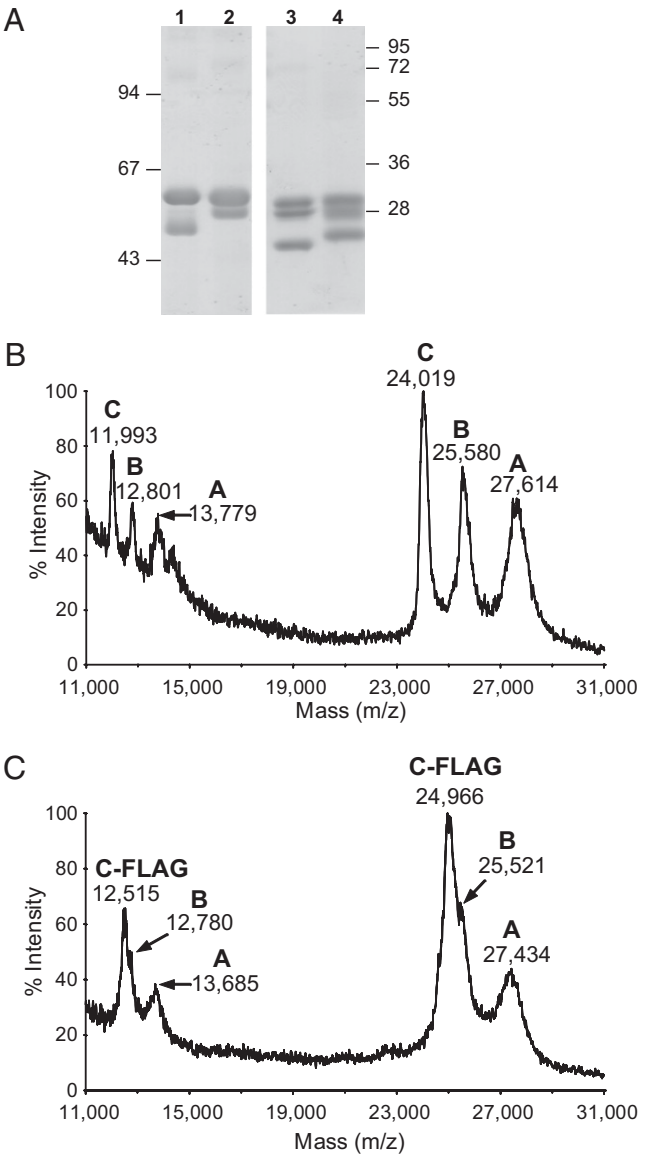


**Fig. 1.** SDS/PAGE and MALDI-TOF mass spectrometry analyses of serum and WT rC1q. (*A*) SDS/PAGE analysis: lane 1, unreduced serum C1q; lane 2, unreduced WT rC1q; lane 3, reduced serum C1q; lane 4, reduced WT rC1q. The molecular weights of unreduced and reduced markers indicated in kDa are shown on the left and right sides, respectively. (*B* and *C*) MALDI-TOF mass spectra of serum C1q (*B*) and WT rC1q (*C*). Analyses were performed on reduced samples as described under *Materials and Methods*. A representative spectrum of four measurements is shown in the case of WT rC1q, and, therefore, the mass values indicated are slightly different from those stated in the text, which represent mean values ±SD of the different measurements.

head domains and the central stalk are clearly visible in most cases. These images are indistinguishable from those obtained using serum-derived C1q (Fig. 2 *C* and *D*) (13), providing strong indication that the expression method used leads to the production of appropriately folded, hexameric C1q molecules.

**Expression of rC1q Variants.** Recent studies are consistent with the hypothesis that assembly of the C1 complex involves major ionic interactions between acidic $Ca^{2+}$ ligands of the C1r and C1s CUB (complement C1r/C1s, Uegf, bone morphogenetic protein) domains and basic residues of C1q putatively corresponding to unmodified lysines located in the collagen-like stems, namely

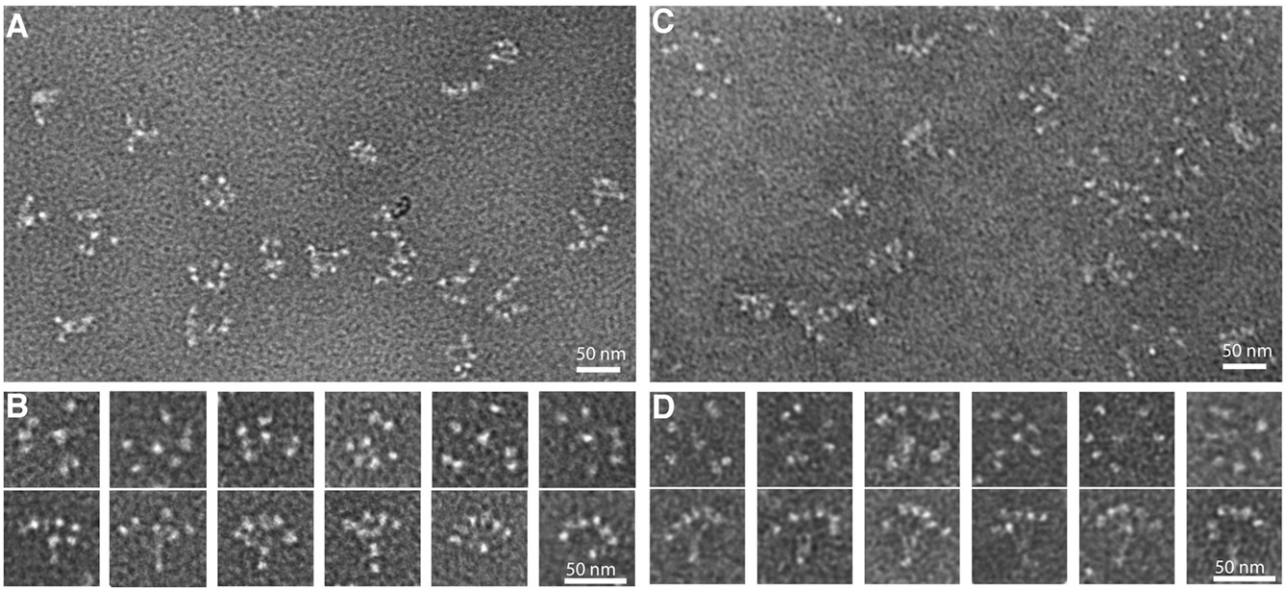


**Fig. 2.** Negative-staining electron microscopy of WT rC1q (*A* and *B*) and serum C1q (*C* and *D*). (*A* and *C*) Overall views. (*B* and *D*) Selected images of individual molecules showing top views (upper row) and side views (lower row). Samples were stained with sodium silicotungstate as described under *Materials and Methods*.

LysA59 and/or LysB61 and/or LysC58 (12, 14–16). With a view to test this hypothesis, these residues were individually mutated to alanine, and recombinant C1q molecules bearing either a single mutation on one of the chains or the three mutations together were expressed and purified as described for WT rC1q. Remarkably, the four rC1q variants readily bound to immune aggregates, indicating that they all retained IgG-binding ability, and their average purification yields were comparable to those observed for WT rC1q. In the same way, analysis of the mutants by SDS/PAGE and electron microscopy yielded similar results compared with native rC1q (Figs. S1 and S2).

**Interaction Properties of WT rC1q and rC1q Variants.** WT rC1q and its variants were immobilized on a sensor chip and their interaction properties were measured by surface plasmon resonance (SPR) using four different soluble ligands: the C1s-C1r-C1r-C1s tetramer, mannan-binding lectin (MBL)-associated serine protease (MASP)-3, IgG, and PTX3. Although probably not a natural C1q ligand, MASP-3 does bind C1q, likely through sites identical or similar to those recognized by C1s-C1r-C1r-C1s in the collagen-like moiety of the protein (16). In contrast, IgG and the long PTX, PTX3, are both physiological ligands of the C1q globular domain (9, 17).

WT rC1q readily bound to both C1s-C1r-C1r-C1s and MASP-3 (Fig. 3 and Fig. S3), with $K_D$ values of 12.5 and 0.66 nM, respectively, similar to the values determined using serum C1q (Table 1). Likewise, rC1q retained the ability of serum C1q to bind IgG and PTX3, again with comparable $K_D$ values. It was clear, therefore, that WT rC1q was fully functional with regard to both the ability of its collagen-like moiety to associate with C1s-C1r-C1r-C1s and the ligand-sensing function of its globular domain.

Introduction of the single mutation LysA59Ala in rC1q resulted in a 10-fold decrease in the binding affinity for C1s-C1r-C1r-C1s that was attributable to a decreased $k_a$ value (Table 1 and Fig. 3*A*). The other two mutations, LysB61Ala and LysC58Ala, each individually abolished the ability of rC1q to associate with C1s-C1r-C1r-C1s, and the same effect was observed using the triple rC1q mutant. In a similar way, the individual mutations of LysB61 and LysC58 each dramatically decreased the interaction of rC1q with MASP-3, whereas mutation of LysA59 only had a slight inhibitory effect compared with the interaction with C1s-C1r-C1r-C1s (Table 1 and Fig. 3*B*). As expected, neither the individual mutations nor the three mutations together had a significant impact on the interaction of rC1q with IgG or PTX3 (Table 1). These experiments,

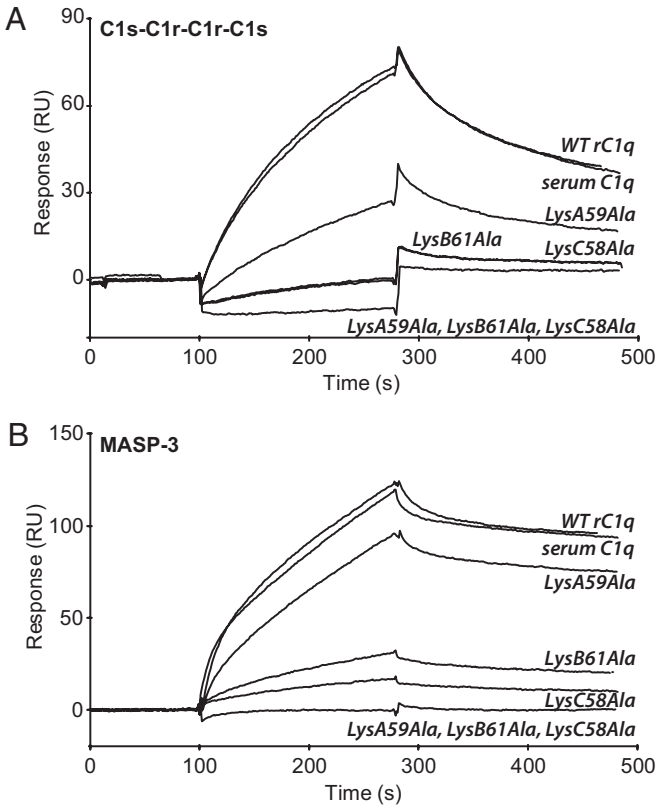


**Fig. 3.** SPR analyses of the binding of C1s-C1r-C1r-C1s (*A*) and MASP-3 (*B*) to immobilized serum C1q, WT rC1q, and rC1q variants. Analyses were performed as described in *SI Materials and Methods*. The C1s-C1r-C1r-C1s and MASP-3 concentration was 18 nM. In *A*, the curves obtained for the LysB61Ala and LysC58Ala mutants are virtually identical and cannot be distinguished.

**Table 1. Kinetic and dissociation constants for binding of C1s-C1r-C1r-C1s, MASP-3, IgG, and PTX3 to immobilized serum C1q, WT rC1q, and rC1q variants**

| C1q samples | C1s-C1r-C1r-C1s | MASP-3 | IgG | PTX3 |
|---|---|---|---|---|
| Serum C1q | | | | |
| $k_a$ ($M^{-1}\cdot s^{-1}$) | $2.64 \times 10^5$ | $3.14 \times 10^5$ | $1.10 \times 10^4$ | $3.23 \times 10^5$ |
| $k_d$ ($s^{-1}$) | $3.52 \times 10^{-3}$ | $4.23 \times 10^{-4}$ | $2.27 \times 10^{-3}$ | $1.13 \times 10^{-3}$ |
| $K_D$ (nM) | 13.3 | 1.35 | 206 | 3.49 |
| WT rC1q | | | | |
| $k_a$ ($M^{-1}\cdot s^{-1}$) | $2.84 \times 10^5$ | $5.94 \times 10^5$ | $1.08 \times 10^4$ | $4.04 \times 10^5$ |
| $k_d$ ($s^{-1}$) | $3.55 \times 10^{-3}$ | $3.94 \times 10^{-4}$ | $1.54 \times 10^{-3}$ | $1.03 \times 10^{-3}$ |
| $K_D$ (nM) | 12.5 | 0.66 | 143 | 2.56 |
| LysA59Ala | | | | |
| $k_a$ ($M^{-1}\cdot s^{-1}$) | $0.27 \times 10^5$ | $2.18 \times 10^5$ | $0.86 \times 10^4$ | $3.41 \times 10^5$ |
| $k_d$ ($s^{-1}$) | $3.48 \times 10^{-3}$ | $5.19 \times 10^{-4}$ | $1.60 \times 10^{-3}$ | $0.91 \times 10^{-3}$ |
| $K_D$ (nM) | 126 | 2.38 | 186 | 2.70 |
| LysB61Ala | | | | |
| $k_a$ ($M^{-1}\cdot s^{-1}$) | ND | ND | $1.07 \times 10^4$ | $3.20 \times 10^5$ |
| $k_d$ ($s^{-1}$) | ND | ND | $1.91 \times 10^{-3}$ | $1.12 \times 10^{-3}$ |
| $K_D$ (nM) | ND | ND | 178 | 3.50 |
| LysC58Ala | | | | |
| $k_a$ ($M^{-1}\cdot s^{-1}$) | ND | ND | $1.01 \times 10^4$ | $2.73 \times 10^5$ |
| $k_d$ ($s^{-1}$) | ND | ND | $1.92 \times 10^{-3}$ | $1.15 \times 10^{-3}$ |
| $K_D$ (nM) | ND | ND | 191 | 4.19 |
| LysA59Ala, LysB61Ala, LysC58Ala | | | | |
| $k_a$ ($M^{-1}\ s^{-1}$) | ND | ND | $0.75 \times 10^4$ | $2.02 \times 10^4$ |
| $k_d$ ($s^{-1}$) | ND | ND | $1.54 \times 10^{-3}$ | $1.02 \times 10^{-3}$ |
| $K_D$ (nM) | ND | ND | 205 | 5.11 |

All $\chi^2$ values ranged between 0.39 and 4.89. ND, not determined because of the low binding level.

thus, provided compelling evidence that two of the targeted lysine residues, LysB61 and LysC58, play a critical role in the interaction of C1q with C1s-C1r-C1r-C1s and MASP-3, establishing that both ligands bind C1q at the same sites and through similar mechanisms involving ionic bonds. The third lysine residue, LysA59, also plays a role in C1 assembly, although to a lesser extent, and is not essential to the interaction with MASP-3.

**C1 Activation Properties of WT rC1q and rC1q Variants.** WT rC1q and its variants were each mixed with the proenzyme C1s-C1r-C1r-C1s tetramer and the resulting complexes were tested for their ability to self-activate upon incubation at 37 °C in the absence of C1 inhibitor. As illustrated in Fig. 4*A*, WT rC1q essentially retained the ability of serum C1q to trigger activation of C1s-C1r-C1r-C1s, yielding 95% activation upon incubation for 1 h. Introduction of the LysA59Ala mutation resulted in a marked increase of the lag phase but did not prevent the activation process. In contrast, the LysB61Ala and LysC58Ala variants, as well as the triple mutant, all lacked the ability to trigger significant activation of the tetramer, yielding values ≤20%, similar to the background activation level measured when incubating the tetramer alone. As expected, addition of C1-inhibitor abolished the activation process in all cases, yielding activation values of 0.5–5% after incubation for 1 h.

We next measured the ability of the rC1q variants to mediate C1 activation by IgG–ovalbumin aggregates in the presence of C1-inhibitor. In line with the self-activation experiments, WT rC1q and, to a lesser extent, the LysA59Ala mutant each yielded activation values comparable to serum C1q upon incubation for 1 h at 37 °C (Fig. 4*B*). Again, the LysB61Ala and LysC58Ala variants and the triple mutant did not trigger significant activation, with values ranging from 5.6% to 9%. These experiments, thus, provided further evidence of the essential role of LysB61 and LysC58 in C1 assembly, confirming that, in contrast, LysA59 is not determinant.

## Discussion

The expression method described in this study, based on stable transfection of HEK 293-F cells and involving fusion of a FLAG tag to the C-terminal end of the C chain, has allowed us to successfully produce human C1q in a recombinant form. The resulting rC1q molecule is obtained with a satisfactory yield and, apart from the C-terminal FLAG tag extension of the C chain, is chemically and structurally similar to serum C1q, as judged from SDS/PAGE, N-terminal sequencing, mass spectrometry, and electron microscopy analyses. A single minor difference is that the mass of the A chain is slightly lower compared with its counterpart in serum C1q, possibly because of the fact that the single N-linked biantennary oligosaccharide borne by this chain lacks a terminal sialic acid residue. Comparative analysis of its interaction properties shows that rC1q fully retains the ability of serum C1q to associate with its cognate proteases C1r and C1s and to recognize physiological C1q ligands such as IgG and PTX3, indicating that both its collagen-like and globular moieties are functional and hence properly folded. Further evidence that rC1q fulfills all functionalities of native human C1q lies in its ability to trigger activation of the C1s-C1r-C1r-C1s tetramer essentially in the same manner as its serum-derived counterpart.

The expression and characterization of rC1q variants carrying mutations of LysA59, LysB61, or LysC58 sheds light on the implication of these residues in the assembly of the C1 complex, establishing that LysB61 and LysC58 each play a key role in the interaction with the C1s-C1r-C1r-C1s tetramer. LysA59 also appears to be involved in the interaction, but likely to a lesser degree. This conclusion is supported by the observations that (*i*) replacement of LysA59 by alanine markedly slows down formation of the C1 complex but does not significantly alter its stability once formed (Table 1) and (*ii*) the LysA59Ala rC1q mutant retains in part the ability to trigger C1 activation, contrary to the LysB61Ala and LysC58Ala variants. Given that the three lysine residues are homologous at the sequence level (10), they are expected to occupy equivalent positions along the collagen-like

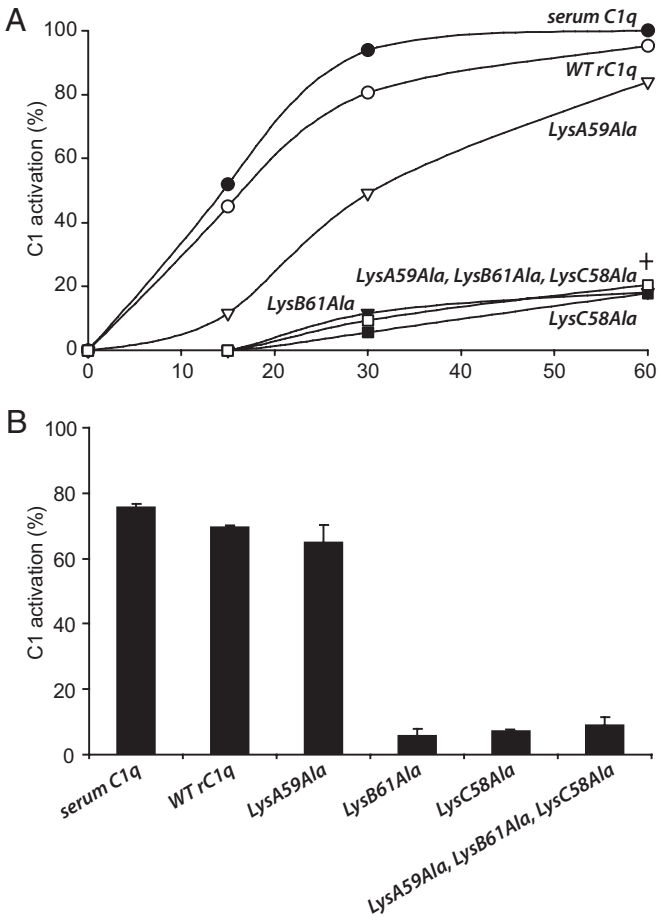


**Fig. 4.** C1 activation by serum C1q and rC1q variants. (*A*) Spontaneous activation. Complexes (0.25 μM) reconstituted from the different C1q samples and proenzyme C1s-C1r-C1r-C1s were incubated for various periods at 37 °C. ▼, LysB61Ala mutant; ■, LysC58Ala mutant; □, LysA59Ala, LysB61Ala, LysC58Ala triple mutant. (*B*) Activation by IgG–ovalbumin immune aggregates. The reconstituted complexes were incubated for 1 h at 37 °C in the presence of 0.2 mg/mL IgG–ovalbumin aggregates and 1 μM C1 inhibitor. The C1 activation extent was measured in each case by SDS/PAGE, followed by Western blot analysis using an anti-C1s antibody (21). In *A*, the background activation level measured when incubating C1s-C1r-C1r-C1s alone for 1 h is indicated by +. Results in *B* are expressed as means ±SD of two independent experiments.

triple helices. Consequently, one of the three side chains is expected to point toward the outside of the C1q molecule, with the other two facing inward and, hence, being more favorably positioned to interact with the tetramer, located inside the C1q cone (2, 9, 12, 14, 16, 18). Thus, a plausible explanation is that the lesser contribution of LysA59 is related to the fact that this occupies the most outer position on the collagen-like stems, a hypothesis fully consistent with the 3D C1q model currently available (2, 9, 12). If this assumption is correct, then the role of LysA59 could be solely to facilitate assembly of the C1 complex by enhancing long-range electrostatic attraction of the negatively charged ligands of the tetramer.

C1s-C1r-C1r-C1s was shown to bind C1q through 6 sites involving the two outer (Glu and Asp) $Ca^{2+}$-coordinating residues of the $CUB_1$ domains of C1r and C1s and $CUB_2$ domain of C1r (14). In each case, these two residues coordinate $Ca^{2+}$ through a single carboxyl oxygen, with their free oxygen being exposed and available for mediating an electrostatic bond with a basic residue (14, 15, 19). Examples of such $Ca^{2+}$-binding CUB domain-mediated salt bridges have been provided by the X-ray structures of the cubilin-intrinsic factor complex (19) and of the MBL–MASP-1 contact region (20). In both instances, each of the two outer acidic $Ca^{2+}$ ligand forms an electrostatic bond with a single basic (Lys or Arg) residue. Thus, each of the six C1q-binding sites of the C1s-C1r-C1r-C1s tetramer is expected to bind a single basic residue contributed by one of the six collagen-like stems of C1q. Our finding that both LysB61 and LysC58 are required to ensure efficient interaction of C1q with the tetramer therefore suggests that either of these residues can be involved, depending on the particular structure of each individual interface. This dual possibility would allow each of the tetramer-binding sites to "choose" the most appropriately positioned Lys on the C1q triple-helix opposite to it, hence facilitating C1 assembly by conferring more flexibility on the interaction. Mutation of either LysB61 or LysC58 would disrupt part of the six tetramer anchor points, thereby preventing efficient interaction.

From a more general standpoint, it should be emphasized that this work establishes that C1q shares with the other defense collagens MBL and ficolins a common mechanism of interaction with its associated proteases, in agreement with previous assumptions (14, 16).

The expression method reported in this study paves the way for deciphering the molecular basis of the multiple binding functions of C1q by mapping the residues involved in the recognition of its numerous targets and receptors. This also makes it possible to produce C1q variants devoid of a particular interaction or sensing property, as exemplified here by the LysB61Ala and LysC58Ala mutants, which both lack the ability to form a stable C1 complex and, therefore, are unable to trigger the classical complement pathway but retain all other C1q binding functions. Such artificial C1q molecules should be of great interest for basic research and biomedical applications.

## Materials and Methods

**Proteins and Reagents.** C1q, proenzyme C1s-C1r-C1r-C1s, C1 inhibitor, and IgGs were purified from human serum, and their concentration was determined as described previously (21, 22). Recombinant human PTX3 and MASP-3 were purified as described previously (23, 24), and their molar concentration was estimated using $M_r$ values of 340,000 (25) and 87,600 (24), respectively. IgG–ovalbumin immune aggregates were prepared at equivalence as described previously (22). Oligonucleotides were purchased from Eurogentec. Restriction and modification enzymes were from New England Biolabs.

**Expression Vectors and Stably Transfected Cell Lines.** The coding sequences of the full-length A, B, and C chains of human C1q were amplified using the VentR polymerase and human cDNA clones purchased from Origene (C1qA, SC 319556; C1qB, SC 119857; C1qC, SC 124311) as templates, according to established procedures. The amplified C1qA, C1qB, and C1qC DNAs were cloned into pcDNA3.1(+) plasmids (Invitrogen) containing neomycin-, hygromycin-, and zeocin-resistance genes, respectively. For expression of the C chain with a C-terminal FLAG epitope (Asp-Tyr-Lys-Asp-Asp-Asp-Asp-Lys), the corresponding DNA sequence was fused to the C1qC DNA by site-directed mutagenesis (Quick Change XL site-directed mutagenesis kit; Agilent Technologies), using the C1qC-containing pcDNA3.1 plasmid as a template. All constructs were checked by dsDNA sequencing (GATC-Biotech).

Freestyle HEK 293-F cells grown in FreeStyle 293 expression medium were cotransfected with the C1qA- and C1qB-containing plasmids using 293fectin, according to the manufacturer's protocol (Invitrogen). Stable transfectants producing both chains were generated, using selection with 400 μg/mL G418 (Invitrogen) and 100 μg/mL hygromycin (Sigma). These cells were then transfected in the same way with the C1qC-FLAG–containing plasmid, and stable transfectants producing the three C1q chains were obtained following additional selection with 10 μg/mL zeocin (Invitrogen).

**Generation of rC1q Mutants.** The LysA59Ala, LysB61Ala, and LysC58Ala mutations were introduced into the corresponding plasmids using the QuikChange site-directed mutagenesis kit (Agilent Technologies) according to the manufacturer's protocol. For the triple mutant, stably transfected cells producing the three mutated chains were obtained as described above for

expression of WT rC1q. The procedures used to generate single mutants are described in *SI Materials and Methods* and Table S1.

**Production and Purification of rC1q.** The C1q-expressing cells were expanded in the Freestyle 293 expression medium (Invitrogen) containing the selection antibiotics and 100 μg/mL L-ascorbic acid (Sigma-Aldrich), and the culture medium was harvested and replaced every 72 h up to three times. WT rC1q and rC1q variants were purified from the culture supernatant using the affinity of C1q for insoluble IgG–ovalbumin aggregates as described for isolation of C1q from human serum (22). The pH of the culture supernatant (500 mL) was adjusted to 7.0 and 8 mL of a 10 mg/mL suspension of immune aggregates was added. After incubation for 45 min at 4 °C, the supernatant was removed by centrifugation and the aggregates were washed three times with 30 mL of 20 mM Tris·HCl, 120 mM NaCl, and 5 mM $CaCl_2$ (pH 7.0). rC1q was eluted by suspending the pellet in 5 mL of 50 mM Tris·HCl and 700 mM NaCl (pH 10.0) and collected by centrifugation. This procedure was repeated once under the same conditions and a third time using 2.5 mL of the elution buffer. The rC1q extracts were dialyzed against 50 mM Tris·HCl and 145 mM NaCl (pH 7.4) and applied to a 3.5 mL anti-FLAG M2 affinity column (Sigma) equilibrated in the dialysis buffer. After washing with 5 mL of the equilibration buffer, the bound material was eluted twice with 3.5 mL of a 100 μg/mL FLAG peptide solution in the same buffer. The eluted fractions were dialyzed against 50 mM triethanolamine·HCl and 145 mM NaCl (pH 7.4) and concentrated to 0.3–0.4 mg/mL. The concentration of purified rC1q was estimated using an absorption coefficient ($A_{1\%,\ 1cm}$) at 280 nm of 0.68 and a $M_r$ value of 467,000, as determined by mass spectrometry.

**N-Terminal Sequencing.** Analyses were carried out after SDS/PAGE and electrotransfer as described previously (26).

**MALDI-TOF Mass Spectrometry.** Analyses were performed on a Voyager DE-STR mass spectrometer (Applied Biosystems) in the positive linear mode as described previously (27). Samples were reduced with β-mercaptoethanol, desalted on a C4 ZipTip (Millipore), and then mixed with a 2,5-dihydroxybenzoic acid matrix in a methanol solution.

**Electron Microscopy.** C1q samples (10 μg/mL) were applied to the clean side of carbon on mica (carbon/mica interface) and negatively stained with 2% (wt/vol) sodium silicotungstate (pH 7.4). A grid was placed on top of the carbon film, which was subsequently air-dried. Images were taken under low-dose conditions with a CM12 Philips electron microscope at 120 kV and a calibrated nominal magnification of 45 K using an ORIUS SC1000 CCD camera (Gatan).

**SPR Analyses.** All experiments were performed at 25 °C on a BIAcore 3000 instrument (GE Healthcare). Details of the procedures used are provided in *SI Materials and Methods*.

**C1 Activation Assays.** The C1 complex (0.25 μM) was reconstituted from purified serum C1q or rC1q variants and the proenzyme C1s-C1r-C1r-C1s tetramer (21). Self-activation was measured by incubating the resulting complexes for various periods at 37 °C in 50 mM triethanolamine·HCl, 145 mM NaCl, and 2.5 mM $CaCl_2$ (pH 7.4). Activation by immune complexes was measured after incubation for 1 h at 37 °C in the same buffer in the presence of 0.2 mg/mL IgG–ovalbumin aggregates and 1 μM C1 inhibitor. The C1 activation extent was determined by SDS/PAGE, followed by Western blot analysis using an anti-C1s antibody (Fig. S4) (21).

**ACKNOWLEDGMENTS.** We thank Jean-Pierre Andrieu for protein sequencing analyses. We acknowledge access to the N-terminal protein sequencing, electron microscopy, and surface plasmon resonance platforms of the Partnership for Structural Biology in Grenoble. This work was supported by French National Research Agency Grant ANR-09-PIRI-0021. C.M. is supported by the laboratoire d'excellence GRAL (ANR-10-LABX-49-01).

1. Cooper NR (1985) The classical complement pathway: Activation and regulation of the first complement component. *Adv Immunol* 37:151–216.
2. Gaboriaud C, et al. (2004) Structure and activation of the C1 complex of complement: Unraveling the puzzle. *Trends Immunol* 25(7):368–373.
3. Bohlson SS, Fraser DA, Tenner AJ (2007) Complement proteins C1q and MBL are pattern recognition molecules that signal immediate and long-term protective immune functions. *Mol Immunol* 44(1-3):33–43.
4. Ricklin D, Hajishengallis G, Yang K, Lambris JD (2010) Complement: A key system for immune surveillance and homeostasis. *Nat Immunol* 11(9):785–797.
5. Ghebrehiwet B, Hosszu KK, Valentino A, Peerschke EI (2012) The C1q family of proteins: Insights into the emerging non-traditional functions. *Front Immunol* 3:52.
6. Nayak A, Ferluga J, Tsolaki AG, Kishore U (2010) The non-classical functions of the classical complement pathway recognition subcomponent C1q. *Immunol Lett* 131(2):139–150.
7. Reid KB (1989) Chemistry and molecular genetics of C1q. *Behring Inst Mitt* (84):8–19.
8. McGreal E, Gasque P (2002) Structure-function studies of the receptors for complement C1q. *Biochem Soc Trans* 30(Pt 6):1010–1014.
9. Gaboriaud C, et al. (2003) The crystal structure of the globular head of complement protein C1q provides a basis for its versatile recognition properties. *J Biol Chem* 278(47):46974–46982.
10. Reid KB (1979) Complete amino acid sequences of the three collagen-like regions present in subcomponent C1q of the first component of human complement. *Biochem J* 179(2):367–371.
11. Reid KB, Thompson EO (1978) Amino acid sequence of the N-terminal 108 amino acid residues of the B chain of subcomponent C1q of the first component of human complement. *Biochem J* 173(3):863–868.
12. Pflieger D, et al. (2010) Analysis of human C1q by combined bottom-up and top-down mass spectrometry: Detailed mapping of post-translational modifications and insights into the C1r/C1s binding sites. *Mol Cell Proteomics* 9(4):593–610.
13. Schumaker VN, Poon PH, Seegan GW, Smith CA (1981) Semi-flexible joint in the C1q subunit of the first component of human complement. *J Mol Biol* 148(2):191–197.
14. Bally I, et al. (2009) Identification of the C1q-binding Sites of Human C1r and C1s: A refined three-dimensional model of the C1 complex of complement. *J Biol Chem* 284(29):19340–19348.
15. Gaboriaud C, et al. (2011) Structure and properties of the Ca(2+)-binding CUB domain, a widespread ligand-recognition unit involved in major biological functions. *Biochem J* 439(2):185–193.
16. Phillips AE, et al. (2009) Analogous interactions in initiating complexes of the classical and lectin pathways of complement. *J Immunol* 182(12):7708–7717.
17. Nauta AJ, et al. (2003) Biochemical and functional characterization of the interaction between pentraxin 3 and C1q. *Eur J Immunol* 33(2):465–473.
18. Brier S, et al. (2010) Mapping surface accessibility of the C1r/C1s tetramer by chemical modification and mass spectrometry provides new insights into assembly of the human C1 complex. *J Biol Chem* 285(42):32251–32263.
19. Andersen CB, Madsen M, Storm T, Moestrup SK, Andersen GR (2010) Structural basis for receptor recognition of vitamin-B(12)-intrinsic factor complexes. *Nature* 464(7287):445–448.
20. Gingras AR, et al. (2011) Structural basis of mannan-binding lectin recognition by its associated serine protease MASP-1: Implications for complement activation. *Structure* 19(11):1635–1643.
21. Tacnet-Delorme P, Chevallier S, Arlaud GJ (2001) Beta-amyloid fibrils activate the C1 complex of complement under physiological conditions: Evidence for a binding site for A beta on the C1q globular regions. *J Immunol* 167(11):6374–6381.
22. Arlaud GJ, Sim RB, Duplaa AM, Colomb MG (1979) Differential elution of Clq, Clr and Cls from human Cl bound to immune aggregates. Use in the rapid purification of Cl subcomponents. *Mol Immunol* 16(7):445–450.
23. Bottazzi B, et al. (1997) Multimer formation and ligand recognition by the long pentraxin PTX3. Similarities and differences with the short pentraxins C-reactive protein and serum amyloid P component. *J Biol Chem* 272(52):32817–32823.
24. Jacquet M, et al. (2013) Deciphering complement receptor type 1 interactions with recognition proteins of the lectin complement pathway. *J Immunol* 190(7):3721–3731.
25. Inforzato A, et al. (2010) The angiogenic inhibitor long pentraxin PTX3 forms an asymmetric octamer with two binding sites for FGF2. *J Biol Chem* 285(23):17681–17692.
26. Teillet F, et al. (2005) The two major oligomeric forms of human mannan-binding lectin: Chemical characterization, carbohydrate-binding properties, and interaction with MBL-associated serine proteases. *J Immunol* 174(5):2870–2877.
27. Tissot B, et al. (2005) Mass spectrometry analysis of the oligomeric C1q protein reveals the B chain as the target of trypsin cleavage and interaction with fucoidan. *Biochemistry* 44(7):2602–2609.